INFLUENCE OF ER DOPING LEVEL AND POST-GROWTH PLASMA TREATMENT ON LUMINESCENCE PROPERTIES OF ZNO NANO- AND MICRORODS

[1]Maksym BURYI, [1]Shelja SHARMA, [2]Zdeněk REMEŠ, [3]Júlia MIČOVÁ

[1]*Institute of Plasma Physics of the Czech Academy of Sciences, Prague, Czech Republic, EU, buryi@ipp.cas.cz, sharma@ipp.cas.cz*

[2]*Institute of Physics of the Czech Academy of Sciences, Prague, Czech Republic, EU, remes@fzu.cz*

[3]*Institute of Chemistry, Slovak Academy of Sciences, Bratislava, Slovakia, EU, Julia.Micova@savba.sk*

https://doi.org/10.37904/nanocon.2025.4983

Abstract

Paper deals with the important question of the influence of plasma treatment on the luminescence properties of the ZnO nano- and microrods especially after the annealing in air at 700 ℃. The annealing in air at 700 ℃ significantly suppresses excitonic luminescence (it is practically vanquished). However, hydrogen plasma treatment makes the excitonic luminescence to raise up again surpassing the initial level of intensity in the as grown sample. The influence of Er content on this effect has been studied. Temperature dependence of the excitonic band has been measured as well on example of the Er doping level at 0.25%. Interestingly, hydrogen plasma treatment applied after the annealing in air at 700 ℃ had strong influence on the excitonic intensity of the photon energy distribution as a function of temperature. Moreover, the effect of annealing in air and subsequent hydrogen plasma treatment on the allowed infrared 1.54 μm erbium transition is quite opposite. Exposure to hydrogen plasma leads after the annealing in air at 700 ℃ to the about double reduction of the 1.54 μm erbium transition. This phenomenon practically does not depend on Er content.

Keywords: ZnO nano- and microrods, plasma treatment, photoluminescence, excitonic band, defects-related band

1. INTRODUCTION

Zinc oxide is one of the most studied materials all over the world, still gaining attention due to its magnificent properties including wide direct bandgap (3.37 eV), high thermal conductivity (50 W/mK) and high exciton binding energy (60 meV at 300 K) [1–3]. Moreover, some other properties give a credit to ZnO creating an added value. These are anticorrosion and antimicrobial abilities [4–7]. Altogether, all of these makes zinc oxide, especially, at the nanoscale a promising material for various applications such as scintillators and nanomedicine [8–11], photovoltaics and photocatalysis [12–14] and many others.

Er supports growth of ZnO in the form of microrods. The larger the Er content (in the sequence 0.05 – 1%) the larger the microrods [15]. This and advanced experimental and theoretical studies led to the conclusion that erbium appears in the form of the Er_xO_y quantum dots serving as nucleation seeds [16].

The luminescence of the ZnO host is composed of the excitonic emission (having maximum at about 3.24 eV) and emission of native defects. The latter is observed within the 1-2 eV spectral region [17,18]. The typical defects in the ZnO nano- and microrods grown using hydrothermal growth are the neutral zinc vacancies (V_{Zn} at about 1.8-2 eV) and zinc dangling bonds (Zn_{DB} at about 2.4 eV) [15]. However, luminescence properties of the hydrothermally grown ZnO are strongly affectable by Er doping.

The red as well as the green bands increase upon the annealing in air at elevated temperatures up to 500 ℃. Further increase of the annealing temperatures led to the slight decrease of the intensity of these bands [15].

Hydrogen plasma treatment results in the enhancement of the exciton-related luminescence band intensity. At the same time the VZn band intensity is decreasing. These processes depended on the Er doping level. The existence of energy transfer between the VZn and zinc interstitial was observed [19].

However, the influence of subsequent air annealing and hydrogen plasma treatment on the luminescence properties of Er doped ZnO nano- and microrods is unknown. This is the aim of the present work

2. EXPERIMENTAL

All of the analytical-grade reagents were used exactly as supplied, requiring no additional purification. Erbium(III) nitrate pentahydrate $Er(NO_3)_3{\cdot}5H_2O$ was obtained from Sigma-Aldrich, while zinc nitrate hexahydrate ($Zn(NO_3)_2{\cdot}6H_2O$) and hexamethylenetetramine (HMTA, $C_6H_{12}N_4$) were acquired from Slavus. A system called So-Safe Water Technologies, which has a conductivity of 0.20 $\mu S{\cdot}cm^{-1}$ at 25 ℃, was used to purify deionized water. The hydrothermal growth method was used to create undoped and Er-doped ZnO nanorods with nominal compositions ZnO:Er (0.05, 0.25, 1%). First, using a magnetic stirrer, 200 ml of deionized water was used to dissolve the equivalent stoichiometric quantities of $Zn(NO_3)_2{\cdot}6H_2O$ and $Er(NO_3)_3{\cdot}5H_2O$, respectively. A Whatman 2 filter was used to filter the prepared solutions. For fifteen minutes, the filtered solutions were mixed and agitated at 400 rpm. In the final suspensions, the ZnO:Er(0.05, 0.25, 1%) had a nominal concentration of 25 mM. A 250 ml aqueous solution of HMTA at a concentration of 25 mM was then made. The solution was filtered through Whatman 2 straight to the $Zn(NO_3)_2{\cdot}6H_2O$ and $Er(NO_3)_3{\cdot}5H_2O$ mixing solutions after being stirred for 15 minutes. After stirring the reaction mixture, nanorods were hydrothermally grown by heating it to 90°C for three hours. After being separated and purified (by removing any remaining salts), the produced nanorods were centrifuged for 15 minutes at 18,000 rpm (RCF: 23,542 ×g) and then rinsed five times with deionized water. The samples were then lyophilized.

A homemade spectrometer containing the following components was used to study the characteristics of photoluminescence (PL): (a) a pulsed ultraviolet (UV) light emitting diode (LED) with a wavelength of 340 nm and a power of 1 mW; (b) a narrow band pass optical filter; (c) a Peltier cooled photomultiplier that is sensitive in the 355-800 nm spectral range (2 nm spectral resolution); (d) a spectrally calibrated double gratings monochromator SPEX 1672; (e) long-pass filters; (f) a lock-in amplifier referenced to the LED frequency (307 Hz).

Luminescence spectra are presented in the energy scale by using the Jacobian correction to convert from wavelength scale.

3. RESULTS AND DISCUSSIONS

UV-visible PL spectra measured in the ZnO:Er(0.05, 0.25 and 1%) samples annealed in air art 700 ℃ are shown in **Figure 1A**. They are composed of at least three contributions/bands appearing at approximately 1.82 eV, 2.4 eV and 3.25 eV. The origin of these bands is neutral zinc vacancy (V_{Zn}), zinc dangling bonds (Zn_{DB}) and excitonic emission (En), respectively [15]. It is known from previous studies [15] that the V_{Zn} in the as grown ZnO:Er(Mo) samples has the tendency to increase upon the annealing temperature reaching maximum intensity in the range 500-700 ℃ (the intensity is doubled as compared to the as grown samples). Moreover, annealing in air is known to strongly reduce or even extinguish the excitonic emission.

The intensity of the V_{Zn}, Zn_{DB} and En bands depends on the Er doping level. The intensity of the V_{Zn} and Zn_{DB} bands remains unchanged in the ZnO:Er(0.05, 0.25%) samples whereas it is about twice as large in the ZnO:Er(1%) sample. In contrast, the weak En band in the ZnO:Er(0.05%) is almost totally suppressed in the ZnO:Er(0.25, 1%). These are expected tendencies reported in [15]. They serve as a reference to the same samples annealed in air at 700 ℃ and subsequently treated by cold Ar + 5%H_2 plasma (see Experimental). The corresponding PL spectra are shown in **Figure 1B**.

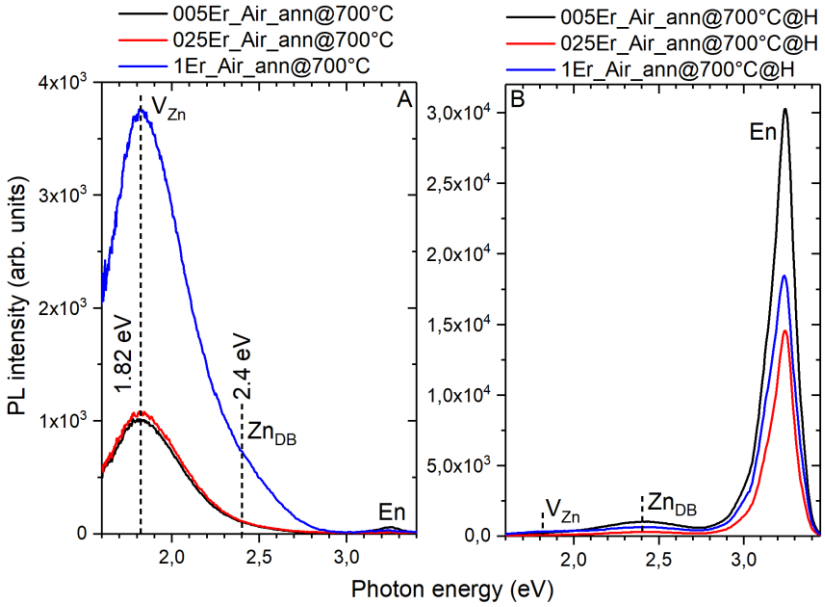

Figure 1 A - UV-visible PL spectra measured in the samples of ZnO:Er(0.05, 0.25 and 1%) annealed in air at 700 ℃ as also indicated in the legend. B - UV-visible PL spectra measured in the samples of ZnO:Er(0.05, 0.25 and 1%) annealed in air art 700 ℃ and subsequently hydrogen plasma treated as also indicated in the legend. En, ZnDB and VZn indicate specific emission bands originating from the excitonic luminescence zinc dangling bonds and neutral zinc vacancy [15].

They exhibit different trends as compared to the only annealed samples. The V_{Zn} band appeared about one order of magnitude suppressed in the ZnO:Er(0.25, 1%) while it was only fivefold weaker in the ZnO:Er(0.05%) after the plasma treatment. Oppositely, the Zn_{DB} band was about one order of magnitude and triple increased in the ZnO:Er(0.05%) and ZnO:Er(0.25%), respectively, while it remained unchanged in the ZnO:Er(1%) after the plasma treatment. This has never been observed before in the as grown samples of ZnO:Er(0.05, 0.25, 1%) nano- and microrods [15].

The En band became visible and very strong after the plasma treatment. The strongest it was in the ZnO:Er(0.05%). It is about twice as weak in the ZnO:Er(0.25,1%) as compared to the ZnO:Er(0.05%) sample.

All of these indicate strong influences of the annealing in air followed by plasma treatment as well as erbium doping. Recently, Er_xO_y-like structures (quantum dots, QD) have been reported to serve as the nucleation seeds for the ZnO nano- and microrods growth [16]. Er is a donor and thus can contribute its electron through the ZnO/Er_xO_y boundary to ZnO. This electron can change the charge balance appearing at a neutral V_{Zn} making it negative. The larger the Er content, the larger the number of donor electrons. Note that it has previously been found that at doping eve of 1% only about one half of the initial erbium remains in the ZnO material. Ar + 5%H_2 plasma is a reductive medium and injects electrons into the structure as well. Therefore, the V_{Zn} band exhibits the observed trends (**Figure 1B**). At the same time, hydrogen should interact with oxygen removing it thus contributing to the Zn_{DB} and oxygen vacancies (V_O) creation. Note that the hydrogen interacting with the surface of ZnO is not only in the form of a molecule (H_2) but it is atomic (H) and ionic (H^+). Therefore, one may expect high reactivity, much higher than in the case of the annealing in the reductive atmosphere. Oxygen is also building element for the Er_xO_y QDs. The lower the amount of these QDs the stronger the effect of hydrogen on the ZnO structure. The influence of the hydrogen plasma on the Er_xO_y QDs in this way can also be proven by measuring infrared PL of the main 1.54 μm Er^{3+} transition in all the samples. Note, that the existence of a shielding effect in ZnO:Er has been discussed in [15].

The IR PL spectra (the main 1.54 μm Er^{3+} transitions) of the samples studied (only annealed in air at 700 ℃ and also subsequently Ar + 5%H_2 plasma treated) are shown in **Figure 2**.

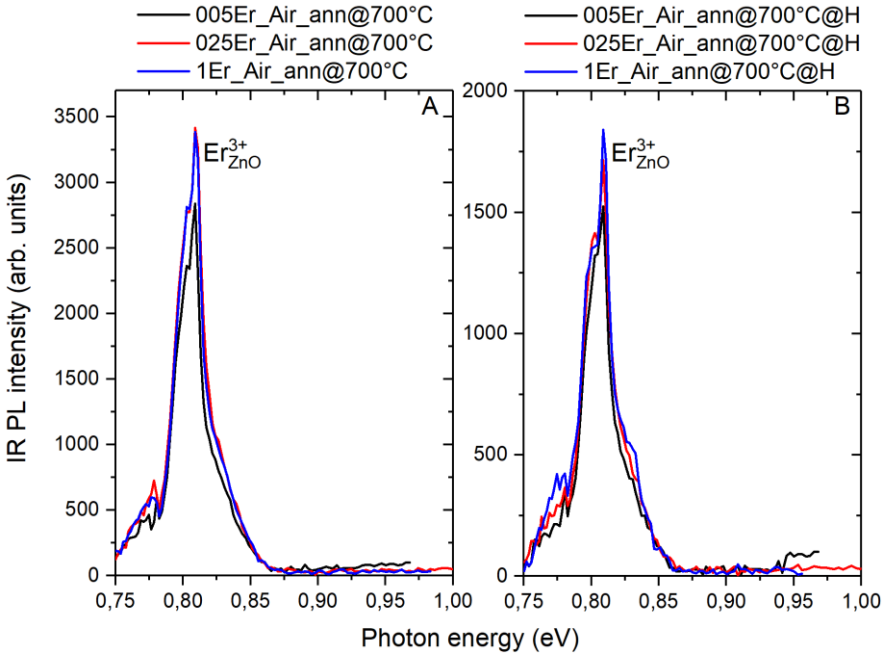

Figure 2 A - IR PL spectra measured in the samples of ZnO:Er(0.05, 0.25 and 1%) annealed in air at 700 ℃ as also indicated in the legend. B - IR PL spectra measured in the samples of ZnO:Er(0.05, 0.25 and 1%) annealed in air art 700 ℃ and subsequently hydrogen plasma treated as also indicated in the legend.

Naturally, the intensity of the main 1.54 μm Er^{3+} transitions is increasing but this trend is very weak in both only annealed and annealed and plasma treated samples. Due to this one may expect energy transfer or upconversion. Note that the maximum energy of the main Er transition is about 0.81 eV. Doubled it corresponds to 1.62 eV – the very beginning of the broad V_{Zn}. Unfortunately, this range is unreachable in the apparatus used (see Experimental). Therefore, the upconversion effect will be studied separately.

Ar + 5%H_2 plasma treatment resulted in the double decrease of the main 1.54 μm Er^{3+} transitions confirming the oxygen removal from the Er_xO_y QDs. Partial reduction of Er^{3+} to metal Er as well as Er^{2+} creation cannot be excluded in this case (see [16]).

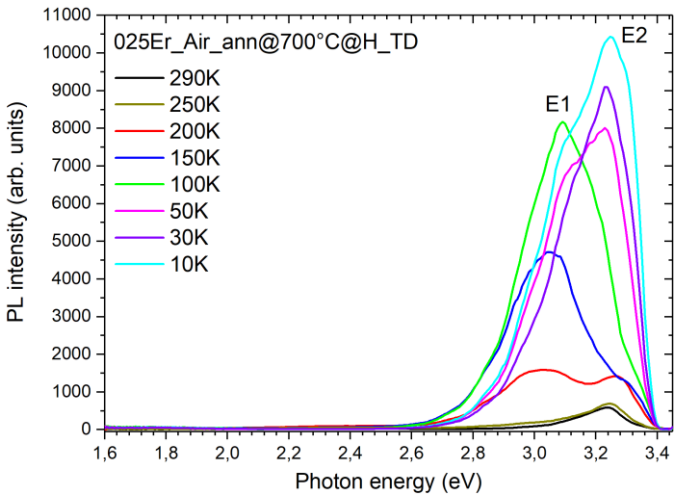

Figure 3 Temperature dependence of the En band measured in the ZnO:Er(0.25%) sample annealed in air at 700 ℃ with the subsequent plasma hydrogenation. E1,2 are specific contributions.

To get better insight into the effect of the plasma hydrogenation on the En band, it has been measured at low temperatures. The corresponding spectra are shown in **Figure 3** on example of the ZnO:Er(0.25%) where the intensity of this band was the weakest among the samples.

It can be seen that the spectrum is composed of at least two complex bands appearing at about 3 eV (E1) and 3.24 eV (E2). The second one originates from excitons. The first one can have the excitonic origin as well as it might have been the interstitial oxygen emission (has maximum at about 2.9 eV) [15]. However, the latter is not probable considering plasma hydrogenation. Hydrogen radicals and ions would rather remove oxygen as discussed above. Therefore, the component E1 is expected to originate from bound excitons and donor-acceptor pairs (DAP).

The E1 band has the tendency to raise as a function of temperature in the range 290-100 K. Then it drops down to the 50-10 K range. The E2 band is increasing in intensity and redshifting to 3.2 eV practically all the time in the 290-10 K range. This indicates the presence of some defects having energy levels at the bottom of the conduction band, most probably, hydrogen. These levels participate in the exciton luminescence processes. Their influence becomes even more pronounced at lower temperatures due to the well-known effect of the bandgap broadening upon cooling. In the case of DAP responsible for the E1 band one could expect electrons to transfer to the excitonic excited states through the hydrogen levels, the effect similar to tunnelling.

4. CONCLUSION

The known observation that the annealing in air at 700 ℃ significantly suppresses excitonic luminescence (3.24 eV) and at the same time improves defects-related red (1.82 eV) and green (2.4 eV) luminescence in the hydrothermally grown ZnO nano- and microrods has been repeated in the present work. Furthermore, the application of Ar + 5%H2 plasma after the annealing resulted in the strong increase of the excitonic emission (several orders of magnitude), suppression of the red (by about one order of magnitude) and improvement of the green emission (by about one order of magnitude). Er doping level had a strong influence on the luminescence intensity of the mentioned bands improving the defects-related and suppressing the excitonic ones. The observed effects were explained by the participation of the ErxOy QDs serving as nucleation seeds for the ZnO nano- and microrods growth in luminescence properties injecting electrons into the ZnO structures. Plasma hydrogenation cuts off some, probably, bridging, oxygen ions from the ErxOy QDs thus at least partly breaking the bonds between ZnO and ErxOy. This has been proven also by measuring IR PL of the 1.54 μm main Er3+ transition – its intensity has been doubly decreased after the plasma treatment. At the same time plasma dopes the material with hydrogen. This was confirmed by measuring the temperature dependence of the excitonic luminescence. There, the clearly observed charge/energy transfer between excitonic states of different origin through donor levels has been observed.

ACKNOWLEDGEMENTS

The financial support of the Czech Science Foundation project No. 24-12872S and the program "Strategy AV 21" of the Czech Academy of Sciences, specifically work package VP 27 Sustainable Energy (Renewable energy resources and distributed energy systems) are gratefully acknowledged

REFERENCES

[1] AWASTHI, K. Ed. *Nanostructured zinc oxide: synthesis, properties and applications*, 1st ed., Elsevier, Cambridge, 2021.

[2] FEDOTOV, A. K., PASHKEVICH, A. V., FEDOTOVA, J. A., FEDOTOV, A. S., KOŁTUNOWICZ, T. N., ZUKOWSKI, P., RONASSI, A. A., FEDOTOVA, V. V., SVITO, I. A., BUDZYŃSKI, M. Electron transport and thermoelectric properties of ZnO ceramics doped with Fe. *Journal of Alloys and Compounds*. 2021, vol. 854, p. 156169.

[3] PASHKEVICH, A. V., FEDOTOV, A. K., PODDENEZHNY, E. N., BLIZNYUK, L. A., FEDOTOVA, J. A., BASOV, N. A., KHARCHANKA, A. A., ZUKOWSKI, P., KOLTUNOWICZ, T. N., KOROLIK, O. V., FEDOTOVA, V. V. Structure, electric and thermoelectric properties of binary ZnO-based ceramics doped with Fe and Co. *Journal of Alloys and Compounds.* 2022, vol. 895, p. 162621.

[4] SÁNCHEZ-LÓPEZ, A. L., PERFECTO-AVALOS, Y., SANCHEZ-MARTINEZ, A., CEBALLOS-SANCHEZ, O., SEPULVEDA-VILLEGAS, M., RINCÓN-ENRÍQUEZ, G., RODRÍGUEZ-GONZÁLEZ, V., GARCIA-VARELA, R., LOZANO, L. M., ELOYR NAVARRO-LÓPEZ, D., SANCHEZ-ANTE, G., CORONA-ROMERO, K., LÓPEZ-MENA, E. R. Influence of erbium doping on zinc oxide nanoparticles: Structural, optical and antimicrobial aktivity. *Applied Surface Science*. 2022, vol. 575, p. 151764.

[5] ASKAR, A. A., SELIM, M. S., EL-SAFTY, S. A., HASHEM, A. I., SELIM, M. M., SHENASHEN, M. A. Antimicrobial and immunomodulatory potential of nanoscale hierarchical one-dimensional zinc oxide and silicon carbide materials. *Materials Chemistry and Physics*. 2021, vol. 263, p. 124376.

[6] SELIM, M. S., EL-SAFTY, S.A., ABBAS, M. A., SHENASHEN, M. A. Facile design of graphene oxide-ZnO nanorod-based ternary nanocomposite as a superhydrophobic and corrosion-barrier coating. *Colloids and Surfaces A: Physicochemical and Engineering Aspects*. 2021, vol. 611, p. 125793.

[7] SELIM, M. S., SHENASHEN, M. A., ELMARAKBI, A., EL-SAEED, A. M., SELIM, M. M., EL-SAFTY, S. A. Sunflower oil-based hyperbranched alkyd/spherical ZnO nanocomposite modeling for mechanical and anticorrosive applications. *RSC Adv.* 2017, vol. 7, p. 21796.

[8] D'AGOSTINO, D., DI GIORGIO, C., BOBBA, F., DI TROLIO, A., ALIPPI, P., CUCOLO, A. M., AMORE BONAPASTA, A. Effects of cobalt substitution on ZnO surface reactivity and electronic structure. *J. Mater. Chem. C* 2019, vol. 7, p. 8364.

[9] OLEJNIK, M., KERSTING, M., ROSENKRANZ, N., LOZA, K., BREISCH, M., ROSTEK, A., PRYMAK, O., SCHÜRMEYER, L., WESTPHAL, G., KÖLLER, M., BÜNGER, J., EPPLE, M., SENGSTOCK, C. Cell-biological effects of zinc oxide spheres and rods from the nano- to the microscale at sub-toxic levels. *Cell Biol Toxicol.* 2021, vol. 37, p. 573.

[10] KAPAT, K., SHUBHRA, Q. T. H., ZHOU, M., LEEUWENBURGH, S. Piezoelectric Nano-Biomaterials for Biomedicine and Tissue Regeneration. *Adv. Funct. Mater.* 2020, vol. 30, p. 1909045.

[11] SIEBERT, L., LUNA-CERÓN, E., GARCÍA-RIVERA, L. E., OH, J., JANG, J., ROSAS-GÓMEZ, D. A., PÉREZ-GÓMEZ, M. D., MASCHKOWITZ, G., FICKENSCHER, H., OCEGUERA-CUEVAS, D., HOLGUÍN-LEÓN, C. G., BYAMBAA, B., HUSSAIN, M. A., ENCISO-MARTÍNEZ, E., CHO, M., LEE, Y., SOBAHI, N., HASAN, A., ORGILL, D. P., MISHRA, Y. K., ADELUNG, R., LEE, E., SHIN, S. R. Light-Controlled Growth Factors Release on Tetrapodal ZnO-Incorporated 3D-Printed Hydrogels for Developing Smart Wound Scaffold. *Adv. Funct. Mater.* 2021, vol. 31, p. 2007555.

[12] YANG, C., ZHAN, S., LI, Q., WU, Y., JIA, X., LI, C., LIU, K., QU, S., WANG, Z., WANG, Z. Systematic investigation on stability influence factors for organic solar cells. *Nano Energy.* 2022, vol. 98, p. 107299.

[13] PEZHOOLI, N., RAHIMI, J., HASTI, F., MALEKI, A. Synthesis and evaluation of composite TiO_2@ZnO quantum dots on hybrid nanostructure perovskite solar cell. *Sci Rep.* 2022, vol. 12, p. 9885.

[14] LAOKAE, D., PHURUANGRAT, A., WANNAPOP, S., DUMRONGROJTHANATH, P., THONGTEM, T., THONGTEM, S. Preparation, characterization and photocatalytic properties of Er-doped ZnO nanoparticles synthesized by combustion method. *International Journal of Materials Research.* 2023, vol. 114, p. 34.

[15] BURYI, M., REMEŠ, Z., BABIN, V., ARTEMENKO, A., VANĚČEK, V., AUBRECHTOVÁ DRAGOUNOVÁ, K., LANDOVÁ, L., KUČERKOVÁ, R., MIČOVÁ, J. Transformation of free-standing ZnO nanorods upon Er doping. *Applied Surface Science.* 2021, vol. 562, p. 150217.

[16] BURYI, M., REMEŠ, Z., HÁJEK, F., KULDOVÁ, K., BABIN, V., DĚCKÁ, K., HEMATIAN, H., LANDOVÁ, L., NEYKOVA, N., HORYNOVÁ, E., REZEK, B. Peculiarities Related to Er Doping of ZnO Nanorods Simultaneously Grown as Particles and Vertically Arranged Arrays. *J. Phys. Chem. C* 2023, vol. 127, p. 22177.

[17] FRODASON, Y. K., JOHANSEN, K. M., BJØRHEIM, T. S., SVENSSON, B. G., ALKAUSKAS, A. Zn vacancy as a polaronic hole trap in ZnO. *Phys. Rev. B* 2017, vol. 95, p. 094105.

[18] LYONS, J. L., VARLEY, J. B., STEIAUF, D., JANOTTI, A., VAN DE WALLE, C. G. First-principles characterization of native-defect-related optical transitions in ZnO. *Journal of Applied Physics.* 2017, vol. 122, p. 035704.

[19] BURYI, M., REMEŠ, Z., BABIN, V., ARTEMENKO, A., CHERTOPALOV, S., MIČOVÁ, J. Cold plasma treatment of ZnO:Er nano- and microrods: The effect on luminescence and defects creation. *Journal of Alloys and Compounds.* 2022, vol. 895, p. 162671.